Environmental Science Processes & Impacts

ROYAL SOCIETY OF CHEMISTRY

PAPER

CrossMark click for updates

Cite this: *Environ. Sci.: Processes Impacts*, 2015, **17**, 1816

Remarkably constant PAH concentrations in Swiss soils over the last 30 years†

Andreas Gubler,*[a] Daniel Wächter,[a] Franziska Blum[b] and Thomas D. Bucheli[b]

Received 23rd July 2015
Accepted 28th August 2015

DOI: 10.1039/c5em00344j

rsc.li/process-impacts

Although polycyclic aromatic hydrocarbons (PAH) are of concern due to their carcinogenic, mutagenic, and teratogenic properties and their ubiquitous occurrence in environmental compartments, only few studies assessed the temporal evolutions of PAH contents of soils over extended time periods. The Swiss Soil Monitoring Network NABO runs long-term monitoring sites resampled every five years since the 1980s. In the present study, soil (0–20 cm) samples collected from 1985 through 2013 at 25 selected monitoring sites were analysed for the 16 priority PAH according to the U.S. EPA and five PAH marker substances. We observed divergent trends for light PAH, such as naphthalene and phenanthrene, compared with heavy PAH, such as benzo[*a*]pyrene and benzo[*ghi*]perylene. Whereas the former showed decreasing concentrations since the late 1980s, no significant trends were found for the latter. Furthermore, the analyses showed that naphthalene contents decreased most strongly at rural sites featuring low population densities, while phenanthrene contents generally decreased most strongly at semi-rural sites. The deviating evolutions of light and heavy PAH were mainly attributed to their differing physico-chemical properties. Temporal evolutions in soils contradict emission inventory data suggesting PAH emissions to decline since the 1980s.

Environmental impact

The present study gives insights into the environmental distribution and fate of polycyclic aromatic hydrocarbons (PAH), particularly into their long-term occurrence in soils. These results might also enhance the knowledge about other semi-volatile persistent organic pollutants. It demonstrates that concentrations of such pollutants in soils may react slowly to changing immissions. Hence, decreased PAH immissions, caused, *e.g.*, by reduced emissions at their sources, are not necessarily (immediately) reflected by soils. The study further illustrates that emission inventories alone are not capable to predict pollutant occurrence in environmental sink compartments. Therefore, observing temporal evolutions of PAH concentrations in recipient matrices such as soils, assured by long-term monitoring programmes, are essential for their proper exposure and risk assessment.

1 Introduction

Polycyclic aromatic hydrocarbons (PAH) are persistent organic pollutants consisting of two or more aromatic rings. They are of major concern because of their carcinogenic, mutagenic, and teratogenic properties and their ubiquitous occurrence in environmental compartments.[1,2] Incomplete combustion of biomass like wood, coal, and liquid fuels is considered as main source of PAH in the environment. Other sources include industrial processes, such as the production of coke, iron, steel, aluminium, and asphalt, volcanic activities as well as biological and diagenetic processes.[3,4] Throughout the late 19th and the first half of the 20th century, anthropogenic PAH emissions increased strongly as a result of growing consumption of biomass and fossil fuels. Estimates suggest that global emissions reached their maximum between 1990 and 2000 and declined ever since. Identical trends are estimated for developing countries, while emissions in developed countries peaked in the early 1970s and dropped by 70% until 2009 due to the implementation of air quality legal standards. Simulations indicate further strong declines in emissions by developed and developing countries over the next decade.[5]

On the large scale, atmospheric PAH deposition is the main pathway into background soils (*i.e.* soils not contaminated by direct immissions through materials like ashes, tar, oil, *etc.*). For agricultural land, inputs *via* recycling fertilisers, such as compost, digestate, presswater, farmyard manure, and sewage sludge may be relevant, depending on the agricultural practice, particularly the used amounts.[6] Atmospheric concentrations and thus PAH deposition are controlled by advection from primary sources (combustion, industry). Secondary sources (particularly re-volatilisation) seem less important.[7] Differing environmental behaviour is observed for the various PAH congeners as a result of their chemical structures.[8] In the

[a]Swiss Soil Monitoring Network NABO, Agroscope, Reckenholzstr. 191, 8046 Zurich, Switzerland. E-mail: andreas.gubler@agroscope.admin.ch; Tel: +41 58 468 76 66

[b]Environmental Analytics, Agroscope, Reckenholzstr. 191, 8046 Zurich, Switzerland

† Electronic supplementary information (ESI) available. See DOI: 10.1039/c5em00344j

atmosphere, heavy PAH (five or more rings) are almost completely particle-bound, while lighter PAH partition between the gas and particulate phase. Consequently, atmospheric transport is more probable for light PAH, whereas heavy PAH show more local and source-driven contamination patterns. Furthermore, light PAH may be re-volatilised and degraded more easily, whereas heavy PAH tend to accumulate in soils and sediments. Temperature and precipitation rate as well as soil characteristics like soil acidity, organic matter fractions, *etc.* strongly influence the mobility (and thus the effective half-live) of PAH in the environment. However, modelling approaches suggest that biodegradation is the most important removal process from soils,[9] although ageing processes may reduce the bioavailability and thus degradability strongly. Overall half-life times in soils are estimated at 2.2 and 8 years for light and heavy PAH, respectively.[9]

The status of PAH soil concentrations was investigated by several surveys at national scales, *e.g.* for the Czech Republic,[10] Estonia,[11] France,[12] the Netherlands,[13] Norway,[14] Poland,[15] Scotland,[16] Switzerland,[17] and the United Kingdom.[14] These surveys confirmed the omnipresence of PAH in soils and reported elevated concentrations for urban, industrial, and semi-rural areas compared with remote and rural areas. For Swiss soil monitoring sites, concentrations of heavy PAH correlated more strongly with population density than those of light PAH; in contrast, concentrations of light PAH correlated more strongly with soil organic carbon (OC) contents compared with heavy PAH.[18] To our knowledge, only few studies addressed the temporal evolution of PAH soil concentrations over extended time periods. Primarily, there are the works by Jones *et al.*[19,20] who analysed samples dating from the mid-1800s to the 1980s originating from one single field of the Rothamsted Experimental Station (England). More recently, Holoubek *et al.*[21] investigated PAH in soils near the Kosetice observatory (Czech Republic) over a period of ten years (1996–2005).

The objectives of the present study are, on the one hand, to assess the temporal evolution of PAH concentrations of Swiss soils, and, on the other hand, to explore similarities and deviations between the trends for individual PAH. Our analyses comprehended soil samples collected from 1985 to 2013 at 25 long-term monitoring sites of the Swiss Soil Monitoring Network NABO resampled every five years.[17] For each site, soil samples originating from five to six sampling campaigns were analysed for the 16 PAH priority substances according to the U.S. EPA (PAH_{16}) and, additionally, five marker substances. This unique data set allowed us to link the observed time trends to the physico-chemical properties of the individual PAH and verify the existing emission inventories of PAH.

2 Methods

2.1. Sampling sites and soil samples

NABO operates about 100 long-term monitoring sites throughout Switzerland. Most of them were sampled for the first time between 1985 and 1989 and re-sampled every five years ever since. For each sampling campaign and site, four replicate samples were collected from the upper part of the soil profile (0–20 cm). In the present study, samples from the first to the most recent sampling campaign were analysed for 25 selected monitoring sites. For each campaign and site, two of the four replicate samples were analysed. Table 1 provides a compilation of site characteristics and expected emission sources, and Fig. 1 depicts their geographical locations. Accounting for possible PAH emission sources and their distances, the sites were classified into urban, semi-rural, rural, and remote (hereafter termed 'exposure classes'). Urban sites are located in or near cities (site 9: Zurich-Dübendorf; 14: Basel; site 97: Lugano); these areas are densely populated and expected emissions mainly originate from industrial areas, construction, heating sources, and traffic. Semi-rural sites are located in rural areas that are relatively densely populated and hold further emission sources like road or railway traffic and/or industrial installations. Large parts of Switzerland's lower areas including the Central Plateau, the Ticino, and the large alpine valleys fall into this category. Rural sites exhibit settlement areas in 1.5 to 3.5 km distance as only direct emission sources. The sole remote site is located within the Swiss National Park at 2400 m above sea level; the road of a mountain pass located in a distance of 1.8 km at an altitude of 1950 m represents the nearest PAH source.

The investigated soil samples are composite samples (0–20 cm soil layer; 25 subsamples taken by a gouge auger of 2.5 cm diameter) representing an area of 10 m by 10 m.[17] Up to the third campaign, the samples were prepared at NABO's former domicile at Bern; all later samples were prepared at our current domicile near Zurich. The samples were oven-dried at 40 °C and subsequently sieved to remove coarse soil components (>2 mm). No relevant losses of PAH occur for drying temperatures up to 40 °C.[23] The drying duration varied from two to four days for the samples of the first three campaigns, whereas the drying duration was standardised at 48 hours for the later samplings. The archived samples were mixed well by a Turbula shaker prior to taking sub-samples for the PAH analyses. The whole process from sampling through lab analysis is standardised by standard operation protocols.

2.2. Chemical analyses

The concentrations of PAH_{16} were determined, namely (in order of increasing molecular weight) naphthalene (NAP), acenaphthylene (ACY), acenaphthene (ACE), fluorene (FLU), phenanthrene (PHE), anthracene (ANT), fluoranthene (FLT), pyrene (PYR), benz[*a*]anthracene (BaA), chrysene (CHR), benzo[*b*]fluoranthene (BbF), benzo[*k*]fluoranthene (BkF), benzo[*a*]pyrene (BaP), dibenz[*a*,*h*]anthracene (DBA), indeno[1,2,3-*cd*]pyrene (IPY), and benzo[*ghi*]perylene (BPE). The sum of these is abbreviated as $\sum PAH_{16}$. Additionally, concentrations of five marker substances were determined: retene (RET), perylene (PER), coronene (COR), 4-*H*-cyclopenta-phenantrene (cPHE), and cyclopenta[*cd*]pyrene (cPYR). Deuterated PAH were used as internal standards. About 10 g of ground soil was spiked with 20 μl containing 200 ng of each of the individual PAH internal standards. The spiked samples were Soxhlet extracted with hexane for 36 hours. Subsequently, the extracts were

Table 1 Site characteristics and PAH emission sources

Exposure class	Site ID	pH[a] ($CaCl_2$)	OC[a] (%)	Altitude (m.a.s.l.)	Population density[b] (inhab. per km^2)	Mean temperature (°C)	Precipitation (mm per year)	Land use[c]	Emission sources	Direction & distance (m) of presumed PAH source(s) relative to site	
Urban	9	5.4 (0.2)	1.3 (0.1)	324	3500	9	790	Crop rotation	Settlement area	W	500
									City centre	N	750
									Industrial quarters	E, NE, N	2000–4000
	14	7.1 (0.1)	2.0 (0.2)	440	2497	7.9	1130	Crop rotation	Industrial quarter & settlement area	N	500
									Airport	NE	2500
									Large-scale firing plant	NW	3000
	97	5.2 (0.1)	2.4 (0.3)	273	1219	11.4	1730	Urban park	City centre	—	0
Semi-rural	5	7.2 (0.2)	2.1 (0.5)	475	142	9.4	1060	Viticulture	Traffic & railway	SE	150
									Settlement area	NE	400
	13	5.4 (0.3)	1.7 (0.1)	455	234	8.5	1270	Crop rotation	Settlement areas	NE, SW, SE	800, 1500, 1500
	24	4.9 (0.2)	3.1 (0.1)	387	612	8.3	1010	Decid. forest	Cement industry	N	1000
									Settlement area	SE	1200
	29	5.5 (0.3)	3.0 (0.4)	450	384	8.3	1160	Crop rotation	Traffic	SW	50
									Industrial quarter	SE	1300
	30	5.0 (0.2)	3.1 (0.1)	635	868	8.3	1160	Grassland	Settlement area	NW	800
									City centre	SW	4000
									Industrial quarter	N	3000
	31	6.0 (0.3)	2.3 (0.2)	775	568	6.8	1150	Crop rotation	Tar recycling plant	W	1500
									Settlement area	W	1500
	33	6.2 (0.3)	5.2 (0.3)	431	232	8.8	1700	Grassland	Traffic	W	200
									Industrial quarter	NW	1000
									Settlement areas	NW, W, S	1000–1500
									Waste incineration plant	NW	3400
	36	5.9 (0.3)	2.4 (0.2)	500	273	8.3	1150	Crop rotation	Large-scale firing plant	NE	500
									Settlement area	NE	500
	38	5.8 (0.3)	2.1 (0.1)	478	251	8.5	1270	Crop rotation	Traffic	NE	200
									Settlement area	NE	400
	44	5.3 (0.4)	1.7 (0.2)	417	652	8.2	1090	Crop rotation	Railway	SW	200
									Industrial quarter	SE	2000

Table 1 (*Contd.*)

Exposure class	Site ID	pH[a] ($CaCl_2$)	OC[a] (%)	Altitude (m.a.s.l.)	Population density[b] (inhab. per km^2)	Mean temperature (°C)	Precipitation (mm per year)	Land use[c]	Emission sources	Direction & distance (m) of presumed PAH source(s) relative to site	
	94	6.2 (0.6)	2.0 (0.0)	209	412	10.6	1920	Horticulture	Large-scale firing plant	S	500
									Settlement areas	SE, SW	1000, 1500
									Industrial quarter	W	2200
	98	6.1 (0.2)	5.0 (0.2)	455	295	8.6	1208	Grassland	Traffic	N	200
									Railway	E	250
									Industrial quarter	S, N	1500, 1800
									Settlement area	S	2500
	102	7.2 (0.1)	1.3 (0.0)	379	231	9.1	881	Crop rotation	Settlement area	NW	800
									Large-scale firing plant	NW	2600
	103	6.3 (0.4)	2.7 (0.1)	431	391	10.1	1015	Crop rotation	Traffic	S	15
									Settlement areas	SW, NE	300, 500
Rural	18	3.3 (0.1)	6.0 (1.4)	525	396	8.1	1170	Conif. forest	Settlement areas	W, N	2000, 2500
	25	7.2 (0.1)	2.8 (0.1)	545	55	8.4	816	Crop rotation	Settlement area	NW	1500
	60	5.4 (0.2)	4.3 (0.3)	955	132	7	1796	Grassland	Settlement area	NW	3500
	62	5.0 (0.2)	4.6 (0.3)	1065	302	5.3	1146	Decid. forest	Settlement area	SW	3000
	83	3.4 (0.1)	6.6 (1.0)	1040	444	5.5	1727	Conif. forest	Settlement area	SE, W	2500, 3000
	85	7.1 (0.1)	6.0 (0.3)	383	432	8.3	890	Decid. forest	Settlement area	SE	2000
	92	3.8 (0.1)	10.7 (0.9)	1080	92	9.2	2277	Decid. forest	Settlement area	SW	2000
Remote	75	5.0 (0.1)	3.9 (0.1)	2400	<1	0.2	722	Conservation area (grassland)	Traffic (mountain pass)	NE	1800

[a] Mean (standard deviation) including all samplings. [b] Population density within a radius of 5 km around the site based on 2013 census data.[22] [c] Grassland only includes sites permanently used as grassland. Fields in crop rotations are temporarily also used as grassland.

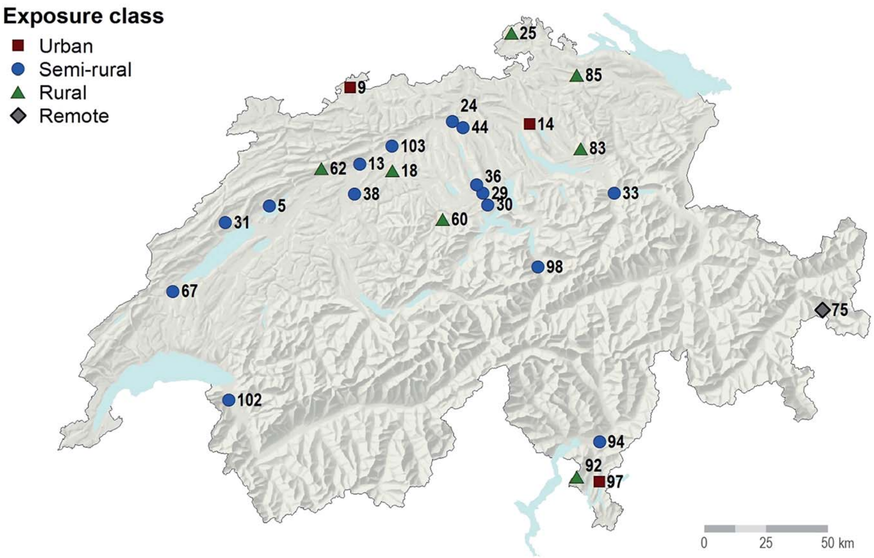

Fig. 1 Location of sampling sites within Switzerland (with site ID) and exposure classes according the expected PAH emission sources and their distances.

concentrated and cleaned in various steps, including liquid–liquid partitioning with dimethylformamide : milli-Q water (9 : 1 v/v) and application to water-deactivated silica gel. Finally, the analysed substances were separated and detected by gas chromatography coupled to electron ionisation mass spectrometry (GC-MS). All steps of the analytical procedure are described in detail in Bucheli *et al.*[24] With each batch of ten soil samples, a control sample and a procedural blank sample were included in the analysis procedure. The samples of the first five sampling campaigns of each site (two samples per campaign) were analysed within the same batch to avoid temporal laboratory bias within the analyses of the same site. The soil samples of the sixth sampling campaign were analysed separately.

2.3. Quality control

The mean of all blanks over the course of the analyses (2009–2013, $N = 30$) was below 0.1 ng g^{-1} for all analysed substances except PHE (0.3 ng g^{-1} dry weight [d.w.]) and NAP (2.3 ng g^{-1} d.w.). The limits of detection (LOD) were calculated according to Keith *et al.*[25] as mean + 3 × standard deviation (sd), the limits of quantification (LOQ) as mean + 10 × sd. An LOD of 1.1 ng g^{-1} d.w. and an LOQ of 3.0 ng g^{-1} d.w. resulted for PHE. For NAP, these limits were estimated at 7.3 and 20 ng g^{-1} d.w., and for $\sum PAH_{16}$, the limits summed up to 11.4 and 32.3 ng g^{-1} d.w. Accordingly, the $\sum PAH_{16}$ concentrations at the remote site 75 as well as those for NAP at some other sites fell in the range between LOD and LOQ and must be interpreted with caution. However, the good agreement, also for NAP, of the results for the two replicate samples per site and time point (see next paragraph) suggests that the estimated LOQ is rather conservative.

The repeatability of the entire process chain from sampling to lab analyses was captured by the relative sd (RSD; sd divided by mean) of the two samples measured per site and time point. For $\sum PAH_{16}$, the RSD fell mostly between 1 and 21% (0.1 and 0.9 quantiles) with a median of 6%. Most of the individual substances showed similar RSD ranges with median RSD from 6 to 9% except ACY, ACE, ANT, RET, PER, and cPHE. The latter showed median RSD from 11 to 15% and 0.9 quantiles between 30 and 50%. In accordance with the concentration-dependent Horwitz function for within-laboratory precision,[26] we attributed the elevated variability to the low concentrations of these substances (*cf.* ESI Fig. S1†). Comparable values were reported by Desaules *et al.*[17]

Two soils served as control samples to assess the variability between different batches (*i.e.* reproducibility). The control samples showed an RSD of 18 and 10%, respectively, for $\sum PAH_{16}$ and an RSD between 10 and 50% for individual substances. However, the values determined for the control samples showed no temporal trends. Accordingly, the performance of the analytical procedures remained stable and the storage duration of the control samples did not alter the PAH contents. In addition, regular successful participation in the International Sediment Exchange for Tests on Organic Contaminants (SETOC[27]) of the Wageningen Evaluating Programmes for Analytical Laboratories (WEPAL) served as external quality control of our laboratory.

2.4. Statistical analyses

PAH concentrations were available for five or six sampling campaigns (10 and 14 sites, respectively). Site 103 was not monitored before 1995; therefore four campaigns only were available. For 10 sites, just one soil sample was collected for the first campaign, and for two sites (38, 97) results of one soil sample only were available for the fifth campaign. In addition, concentrations of some PAH substances are not available for some samples because the levels where below the LOD. The mean of the two samples per site and campaign was used for the statistical analyses. Exploratory plots suggested that PAH concentrations were log-normal distributed; hence, their decadic logarithm was used instead. As OC contents are known for all samples, we considered to normalise the PAH concentrations to OC contents. We rejected this transformation because (i) it did generally not reduce the noise in the temporal evolutions, (ii) a previous study[18] suggested that not all PAH were in equilibrium with the organic matter fraction of the NABO soils, and (iii) OC contents were not necessarily constant over the considered period of 30 years.

The evolution of $\sum PAH_{16}$ concentrations was assessed by fitting a linear regression separately for every site according to eqn (1) using the lmList-function of the lme4 package:[28]

$$\log_{10}(y_{i,t}) = \alpha_i + \beta_i t + \gamma_i u + \varepsilon_{i,t} \quad (1)$$

The left hand term $y_{i,t}$ represents the concentration at site i for the time point t (expressed as sampling campaign; $t = 1, 2, \ldots, 6$). The parameters α and β represent intercept and slope. In addition, the term $\gamma_i u$ accounts for the sudden shift observed at various sites between sampling campaigns 3 and 4 (see below for discussion). The auxiliary variable u is defined as 0 for $t \leq 3$ and 1 for $t > 3$. The results of the third sampling campaign for sites 18, 83, and 92 were discarded for the linear regression because these values are considered erroneous due to a sampling artefact (see Section 3.1 for an explanation). Finally, $\varepsilon_{i,t}$ represents the residuals. Student's t-test was used to assess whether the resulting slopes β_i and the estimates for the shift term γ_i deviated significantly from 0. Generally, a significance level of 0.01 was applied. Residual analyses revealed that the errors of the repeated measurements per site seemed to be independent and no serial correlation was expected between different time points. In a second iteration, similar models were calculated individually for all 21 substances. Models were recalculated excluding the term $\gamma_i u$, if γ_i did not differ significantly from zero for the respective substance.

To assess more in detail which PAH substances showed similar temporal evolutions, the log-transformed concentrations of the 21 PAH substances were centred: for each site and substance, the mean over the whole time series was subtracted from the concentrations of the individual sampling campaigns. The resulting five to six data points (delta concentration values) per site and substance were analysed by a robust principle components analysis (PCA) using the ROBPCA algorithm[29] implemented in R by the function PcaHubert of the rrcov package.[30] The input variables were not scaled to uniform variance prior to PCA.

The slopes β_i derived by the linear models were compared with site characteristics, namely soil acidity (pH), soil OC (mean of entire time series per site), annual mean precipitation and temperature, land use (crop rotation, permanent grassland, forest, and other), and the exposure classes (urban to remote) derived for the present study. Furthermore, the slopes were compared with the respective PAH concentrations of the fifth sampling campaign. To detect groups of monitoring sites with similar temporal evolutions, hierarchical clustering[31] was conducted and illustrated by a heatmap. We used agglomerative clustering based on Euclidian distances (R function hclust). The slopes per site for NAP, PHE, FLT, BaP, and BPE were used as input. There are two reasons for restricting the clustering to these five substances: on the one hand, some of the remaining substances show more noisy data and thus less reliable estimates for their slopes due to low concentrations; on the other hand, medium to heavy PAH would be highly over-represented when using all data leading to a clustering mainly influenced by these. By using the five selected substances, light and heavy PAH equally influence the clustering. Furthermore, site 33 was discarded for clustering because its temporal evolutions are poorly reflected by the chosen model (*cf.* last paragraph of Section 3.3). Analyses and graphics were conducted using the statistical software R[32] including the R packages lattice,[33] ggplot2,[34] and those mentioned above.

3 Results & discussion

3.1. Quality assurance

The good repeatability of each substance's measurements per site and campaign confirms the robustness of the analytical procedures (*cf.* Section 2.3). Blank problems are not relevant; the repeatability of the measurements for NAP and PHE (whose concentrations varied most over the considered time period) were comparable to those of the other PAH. Nevertheless, peculiar patterns within some of the temporal evolutions (see below) indicate the presence of artefacts introduced by processes other than analytics. On the one hand, certain forest sites (18, 83, 92) show unexpectedly high contents for all PAH substances and OC for the third sampling campaign. On the other hand, $\sum PAH_{16}$, PHE, ACE, and FLU show a pronounced decline between the third and the fourth sampling campaign for roughly half of the sites (25, 29, 33, 36, 38, 44, 60, 62, 83, 75, 92, 94). The observed patterns were attributed to issues related with soil sampling and sample pre-treatment. However, modifications of the statistical models allowed capturing these patterns mathematically, as the following paragraphs will show.

Firstly, the concentrations observed at certain forest sites (18, 83, 92) for the third sampling campaign were considered as

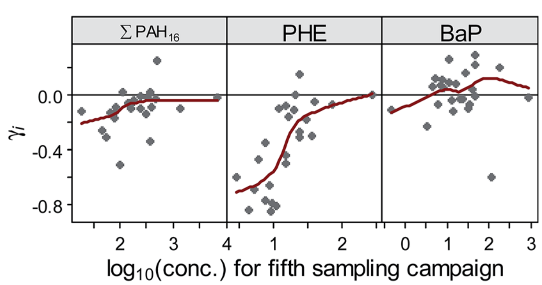

Fig. 2 Estimates of the model parameter γ_i (eqn (1)) reflecting the shift in PAH contents between the third and the fourth sampling campaign for the sum of 16 PAH ($\sum PAH_{16}$), phenanthrene (PHE), and benzo[*a*]pyrene (BaP). Estimated γ_i are plotted *versus* log-transformed concentrations measured at the fifth sampling campaign (solid line: loess-smoother).

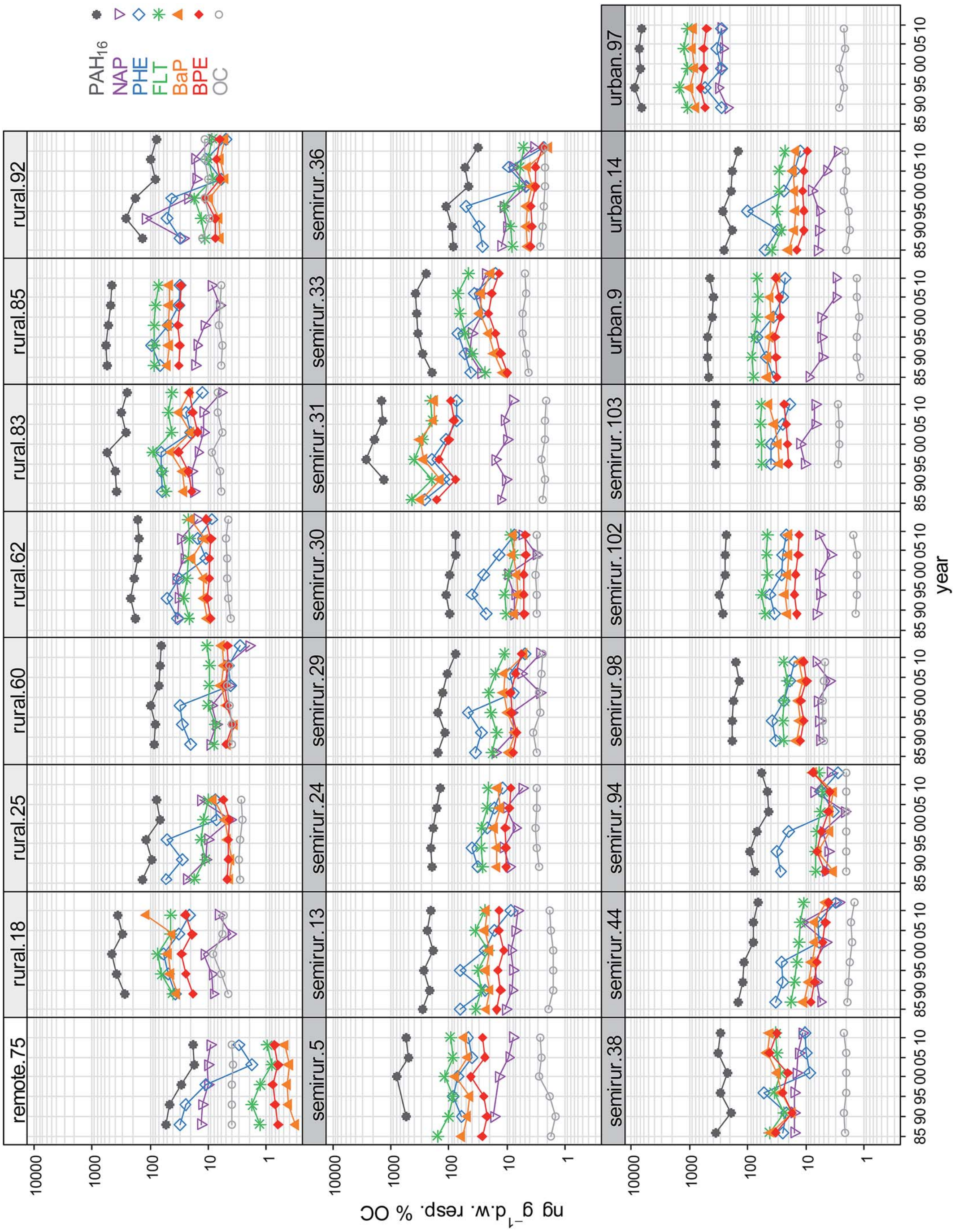

Fig. 3 Concentrations of the sum of 16 U.S. EPA PAH ($\sum PAH_{16}$), naphthalene (NAP), phenanthrene (PHE), fluoranthene (FLT), benzo[*a*]pyrene (BaP), benzo[*ghi*]perylene (BPE), and organic carbon (OC) measured for samples collected from 1985 to 2013. Displayed values represent mean values of two measurements per site and sampling.

statistical outliers and were not used in the linear models. Based on our current knowledge, it seems most probable that these artefacts resulted from deviating soil water status at the time of sampling which may affect the composition of the soil samples if a fixed sampling depth is used.[35] Secondly, the patterns found for $\sum PAH_{16}$ and PHE indicate a change between the third and fourth sampling campaign. The term $\gamma_i u$ was added to the linear models (eqn (1)) to account for the elevated concentrations prior to the fourth sampling campaign. These deviated significantly from zero for $\sum PAH_{16}$ (*p*-value of two-sided *t*-test: 0.001) and the light congeners ACE (<0.001), FLU (0.010), and PHE (<0.001). For NAP, PER, and COR, *p*-values (0.023 to 0.045) indicated weak significances, while deviations for all remaining congeners were non-significant. Consequently, the term $\gamma_i u$ was removed from the regressions for all substances except $\sum PAH_{16}$, ACE, FLU, and PHE to avoid

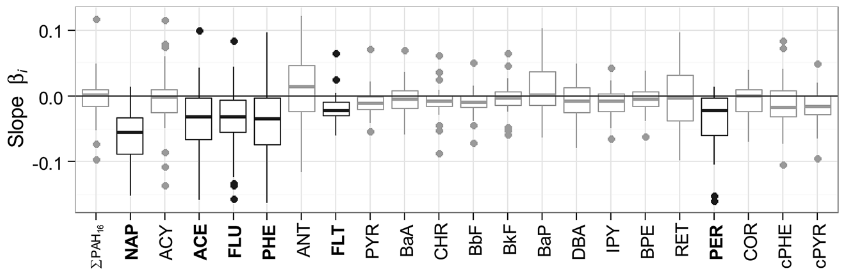

Fig. 4 Estimates of the model parameter β_i (eqn (1)) reflecting the linear temporal trend. Boxplot per substance ($N = 25$); for highlighted substances, β_i deviates significantly from 0 (two-sided t-test at a significance level of 0.01). See Section 2.2 for the abbreviations used for the substances.

distortion of the trend estimates. However, it seems unlikely that the observed sudden drops were caused by real changes, particularly because they coincide with the modification in the drying duration of the samples and the relocation of the laboratory (*cf.* Section 2.1): the longer drying duration applied at the beginning coincides with elevated concentrations of several light PAH. Cousins *et al.*[36] demonstrated that soil samples might be increasingly contaminated from exposure to laboratory air during drying, especially within the first days. Contamination occurred only for ACE, FLU, and PHE, but not for heavier PAH. In addition, the more soil concentrations fall below the thermo-dynamic equilibrium with respect to the laboratory air, the higher PAH transfers into the samples are expected.[37] Indeed, sites with low concentrations showed the most pronounced drops (Fig. 2). Hence, the elevated concentrations prior to the fourth sampling campaign were most likely induced by the longer drying durations (Fig. S2† provides time series corrected for the shift γ_i). In addition, the relocation might have had an effect, possibly the two laboratories varied with respect to PAH air concentrations.

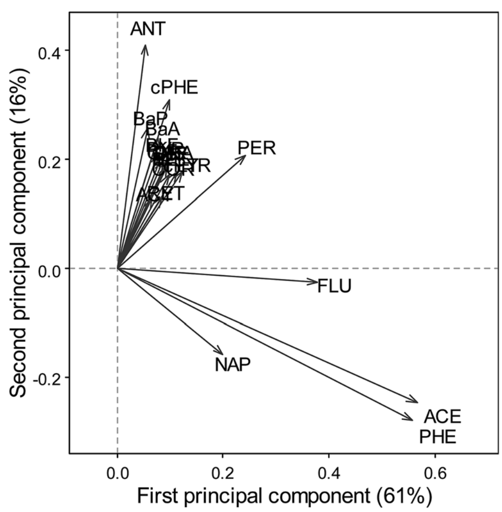

Fig. 5 Loadings of the first two principal components (explained variance in brackets) derived by robust PCA based on log-transformed data centred per site and substance (delta concentration values per time point with respect to the means per site and substance). See Section 2.2 for the abbreviations used for the substances.

3.2. PAH soil concentrations and trends 1985–2013

Representative for the studied PAH, the concentrations of NAP, PHE, FLT, BaP, BPE, and $\sum PAH_{16}$ from 1985 to 2013 are presented in Fig. 3 (for the remaining substances, see Fig. S3 and S4†). The lowest $\sum PAH_{16}$ concentrations were found at the remote site 75 (19 ng g^{-1} d.w. in 2008), whereas the urban site 97 exhibited the highest contents (6870 ng g^{-1} d.w. in 2009). Rural, semi-rural and the remaining urban sites did not differ substantially with respect to PAH concentrations. Relative contributions of light PAH are expected to rise with increasing distance to PAH sources[8] and decreasing population density.[18] In fact, the remote and rural sites show increased shares of NAP and PHE accounting together for 30–80% of $\sum PAH_{16}$. In turn, their shares are generally low at urban sites (<15%).

Regarding the variations over time, substantially decreasing concentrations were observed at most sites for NAP, PHE, and consequently for $\sum PAH_{16}$. Considering the geometric means of the 22 sites with complete data for the sampling campaigns one to five (all sites except 5, 31, and 103), concentrations of $\sum PAH_{16}$ dropped from 215 to 169 ng g^{-1} d.w. from the first to the fifth sampling. For NAP and PHE, concentrations dropped from 13.3 to 10.0 and from 39.4 to 14.0 ng g^{-1} d.w., respectively. In contrast, the geometric mean of FLT concentrations decreased only slightly from 24.9 to 22.6 ng g^{-1} d.w., whereas those of BaP and BPE fluctuated around 14 and 11 ng g^{-1} d.w., respectively. Medium to heavy PAH (including FLT, BaP, and BPE) showed congruent evolutions per site indicating no general trend; however, increasing (sites 33 and 103) and decreasing (9, 14, 24, 31, 36, 44) trends occurred at single sites.

The slopes β_i of individual sites, a proxy for the respective temporal trends, are displayed per substance in Fig. 4. The estimated slopes for NAP, ACE, FLU, PHE, and PER fell between −0.1 and 0 for most sites and deviated significantly from zero (p-values of t-test: <0.001, 0.004, 0.007, 0.001, and 0.001). Furthermore, most slopes for FLT were between −0.05 and 0; their deviation from zero was significant as well (p-value: 0.001). In contrast, the null-hypothesis $\beta = 0$ could not be rejected for $\sum PAH_{16}$ and all remaining congeners. Accordingly, concentrations of the studied soils largely remained stable over the considered period of 25 years, except for light PAH and PER as well as for few exceptional sites.

To assess the similarities in the temporal evolutions of individual PAH in more detail, the PAH concentrations centred per site and substance (delta concentration values) were inspected applying a robust PCA. The first two principle components, explaining roughly 60% and 16% of the total variance, are displayed in Fig. 5. For the first component, the highest loadings were observed for PHE and ACE followed by FLU, implying that relative concentration changes were highest for these. For NAP and PER, considerably smaller, but still elevated loadings were observed. The second component shows negative loadings for NAP, PHE, ACE, and FLU and positive loadings for all remaining PAH including ANT, ACY, all heavy PAH, and marker substances. Fig. 3 clearly indicates deviating temporal trends for the latter group compared with the former group of light PAH. Furthermore, high (but opposite) loadings for RET and PER on the third component (data not shown) indicate temporal trends slightly deviating from those of the group of heavy PAH.

In a previous study, Brändli *et al.*[18] obtained a similar clustering of PAH congeners for immission profiles derived by linear un-mixing: one profile showing high portions of NAP, PHE, ACE, and FLU (light profile), and two further profiles showing high portions of ACY, ANT, and heavy PAH (heavy profiles). These profiles were based on PAH concentrations of 105 NABO monitoring sites determined for the third sampling campaign. It was assumed that the immission profiles might be induced by increasing distance to PAH sources, because atmospheric transport is more probable for light PAH.[8] Heavy PAH have more local, source-driven contamination patterns:

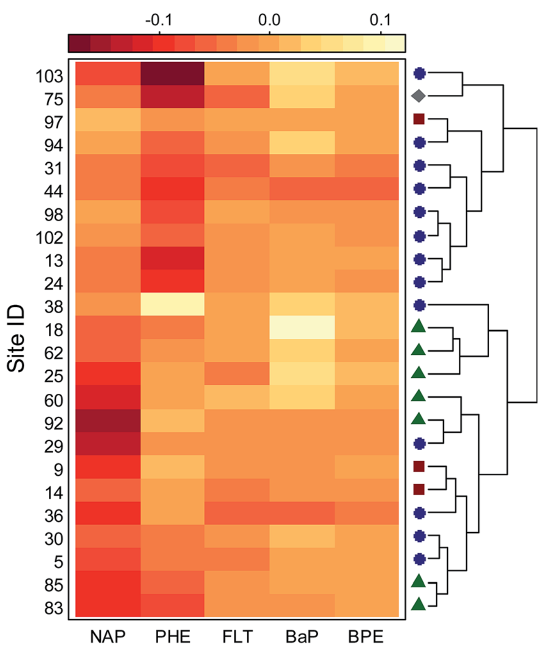

Fig. 6 Heatmap and dendrogram of hierarchical clustering based on the slopes per site and substance for naphthalene (NAP), phenanthrene (PHE), fluoranthene (FLT), benzo[*a*]pyrene (BaP), and benzo[*ghi*]perylene (BPE). The hues represent the estimated slope β_i with darker hues representing more negative slopes (colour key on top). The symbols on the right represent exposure classes (diamond: remote; triangle: rural; circle: semi-rural; rectangle: urban). Site 33 was not considered as the slopes poorly reflect its temporal evolutions.

concentrations of PAH in air,[38] snow,[39] and soil[40,41] were considerably decreasing with increasing distance to busy roads – with more pronounced decreases for heavy PAH. Hence, the light profile presumably reflected the immissions at sites in a larger distance to PAH sources compared with the heavy profiles. However, the immission profiles might as well represent different groups of PAH emission sources instead of increasing distance to them. According to Brändli *et al.*[18] the light profile possibly reflected emissions from biomass burning, especially of wood. According to Swiss inventory data,[42] the latter represented by far the most important PAH source on the national scale attributing for 78% of the emissions in 2012. Considering the decreasing concentrations of light PAH in soils, it seems tempting to attribute the observed concentration changes of particularly the compounds indicative of this source to changes in biomass burning. Whether or not the temporal development of PAH in Swiss soils reflects changes for specific emission sources or emissions in general will further, and more conclusively, be discussed below.

3.3. Similarities and differences between sites

The slopes β_i derived per substance and site were further assessed to detect similarities and discrepancies between sites. Compared with the general trends, site 33 showed the most deviating temporal evolutions; these were inadequately reflected by the used linear model and will be discussed separately at the end of this section. The slopes of the remaining sites were assessed by hierarchical clustering.

Considering the hierarchical clustering and the corresponding heatmap (Fig. 6), we notice first the division into two subgroups: one group (sites 103 through 24) generally showed most decreasing trends for PHE, whereas the second group (sites 38 through 83) exhibited most negative trends for NAP. The further clustering into smaller groups mainly seemed to be ruled by differences between the slopes of the medium to heavy congeners FLT, BaP, and BPE. Interestingly, all rural sites fell into the cluster showing more negative NAP slopes. This cluster further included two of the urban and five semi-rural sites. The cluster showing more negative PHE slopes mainly consisted of semi-rural sites, the urban site 97, and the remote site 75. As discernible in ESI Fig. S5,† the slopes estimated for NAP were clearly more negative for rural compared with semi-rural and urban sites. In contrast, the slopes for PHE were more negative for semi-rural compared with rural and urban sites. For BaP, slopes were increasingly more negative from rural to semi-rural to urban sites, but there seemed to be no significant difference between any of the classes. Hence, reductions in soil concentrations were most remarkable for NAP at rural and for PHE at semi-rural sites.

The simplest explanation of the observed clustering is indeed the exposure classes respectively the criteria they are based on: from urban to semi-rural to rural sites, distances to possible PAH sources were increasing. For the studied sites, population density was decreasing in the mentioned sequence, while altitude was increasing. To assess the influence of further site characteristics, the slopes of NAP, PHE, and BaP (as representative for heavy PAH) were compared with site characteristics and the PAH concentrations measured at the most recent soil sampling (Fig. S6†). For neither of the three substances, the slopes correlated with the concentrations. Accordingly, the degree of contamination seemed not to have a substantial influence on the slopes. For NAP, more negative slopes coincided with low population densities, higher altitudes, and elevated OC contents. Due to its definition, rural sites showed low population densities. In addition, altitude and the logarithm of population density were inversely correlated (Pearson's correlation coefficient $r = -0.36$), whereas altitude and the logarithm of OC contents were positively correlated ($r = 0.6$; all r were calculated excluding the remote site 75 due to its outlying characteristics; thus, $N = 24$). Hence, the observed patterns with respect to NAP slopes may be explained by direct or indirect correlations with population density and comply with the results of the hierarchical clustering. Although annual mean temperature was strongly correlated with altitude too ($r = -0.72$), the relationship between NAP slopes and temperature seemed less clear due to the large scatter. Hence, whereas the cold condensation process generally leads to elevated fractions of light PAHs at higher altitudes in different matrices,[18,43] and should, accordingly, cause temporarily more stable trends for these chemicals, it does not seem to be the most determining process for temporal changes in the Swiss NABO soils. No obvious patterns were observable with respect to soil pH and annual precipitation. For PHE and BaP, the slopes showed no correlation with neither of the assessed parameters except BaP slopes *versus* population density: slightly positive slopes predominated in sparsely populated areas, while slightly negative slopes prevailed in more densely populated areas. Possibly, the found pattern was random as there is no obvious explanation.

Although land use and vegetation influence PAH deposition (*e.g.* higher fractions of semi-volatile PAH in forests[7]), we found no evidence for land use inducing divergent temporal evolutions (Fig. S7†). The gradient observed for NAP with most negative slopes for forest sites and slopes near zero for urban parks arose from the correlations between population density and altitude with land use: in Switzerland, forest sites are generally found in areas at higher altitudes and/or lower population densities. Generally, grassland and cropland sites did not show contrasting evolutions compared with the remaining sites, although the agricultural practice implies an additional PAH source: recycling fertilisers. If the nutritional requirements were completely supplied with these (based on a standard fertilisation), PAH fluxes into soils comparable to those by atmospheric deposition are estimated for compost, digestate, and presswater, whereas lower input fluxes are expected for farmyard manure and sewage sludge.[6] However, only minor PAH accumulation in soils is expected for standard agricultural practices commonly applied by Swiss farmers as rough mass flux calculations suggest; for instance, applying 150 m^3 per ha per year of manure (9% solid content) containing 13 ng g^{-1} d.w. BaP induces an increase of 1 ng g^{-1} d.w. after 10 years for the top 20 cm of soil (soil bulk density: 1 g cm^{-3}; PAH concentrations of manure by Berset & Holzer[44]). Besides, the application of sewage sludge was prohibited and ceased between 2006 and 2008 in Switzerland. Currently, there is no evidence that input *via* recycling fertilisers affected PAH evolutions substantially at the studied sites; particularly, it cannot explain the increases observed for BaP at the cropland sites 25, 38, and 103.

As evident from Fig. 3, site 33 showed contrasting evolutions for medium to heavy PAH, while evolutions for light PAH (NAP to PHE) were comparable to those of other semi-rural sites. Topsoil concentrations of heavy PAH increased steadily from the first sampling in 1986 until the fourth sampling in 2001. Thereafter, concentrations stagnated or slightly decreased until the following sampling five years later. Until the sixth sampling in 2011, concentrations for all heavy PAH had clearly declined. For instance, BaP concentrations rose from 12 to 30 ng g^{-1} d.w. between 1986 and 2001, then they diminished to 28 ng g^{-1} d.w. in 2006 and 19 ng g^{-1} d.w. in 2011. $\sum PAH_{16}$ accounted for 195, 363, and 248 ng g^{-1} d.w. in 1986, 2001, and 2011, respectively. We mainly attribute both the initial increase as well as the trend reversal after 2001 to the waste incineration plant (KVA Linth) located at a distance of 3.4 km in north-western direction of the monitoring site. Due to the topography, the wind blows predominately in south-eastern and north-western direction, implying that the plant's emissions are likely to reach the monitoring site. The plant started operating in 1973 and was extended in 1984 by a second incineration line. In 2000, the plant was renewed completely and equipped with a state-of-the-art flue gas cleaning system.[45] These measures diminished emissions to the atmosphere dramatically. Although the amount of incinerated waste doubled after the renewal, the masses of dust and NO_x released into the atmosphere declined by 80% according the state's air pollution inventory.[46] The release of PAH was not investigated in this case, but it is known that waste incinerators emitted considerable amounts prior to the establishment of efficient flue gas cleaning.[47] The reported PAH emissions vary strongly (0.9–6000 μg m^{-3} flue gas); they particularly are elevated during the start-up of the incinerator. Assuming average $\sum PAH_{16}$ emissions of 500–1000 μg m^{-3} flue gas and an even deposition over an area of 100 km^2, an hypothetical accumulation in the range of 150–380 ng g^{-1} results after 15 years for the top 20 cm soil layer (bulk density of fine earth, 0.83 g cm^{-3}, and flue gas emissions, 320–420 Mm^3 per year, are known; PAH degradation and losses were neglected). Hence, these over-simplistic estimations support the assumptions that, on the one hand, waste incinerator emissions caused the observed increases of heavy PAH concentrations prior to 2000, and on the other hand, reduced emissions in combination with loss processes such as degradation and particle-bond transport induced decreasing concentrations thereafter. However, it remains unclear why decreasing soil concentrations for heavy PAH were not observed at other sites. It may be speculated that the PAH found at this site are (on average) more recent than at other sites where ageing processes might have reduced the degradability of PAH more strongly. The results of this site confirm that heavy PAH show relatively local, small-scale contamination patterns. For other sites that represent special cases (*i.e.*, 75, 97, 103), the interested reader is referred to the ESI.†

3.4. Comparison with literature and emission inventory data

The long-term evolution of PAH immissions in Switzerland was assessed by profiles of an ombrogenic bog[48] and of lake sediments.[49] Both studies suggested a peak roughly between 1930 and 1950 and a strong decrease thereafter. These findings are in good agreement with soil concentrations reported for the Rothamsted Experimental Station (England):[20] while 19th century samples showed concentrations similar to those measured nowadays at remote sites, total PAH found in the plough layer quintupled throughout the 20th century with more pronounced increases for heavy PAH (>15-fold for BaP, BbF, BkF, and PER) and no or only slight increases for light PAH. The largest part of the concentration increases occurred between 1914 and 1944. Similar temporal evolutions must be expected for Swiss soils in urban and semi-rural areas, presumably also in rural areas.

More recently, Holoubek *et al.*[21] investigated the temporal trends of PAH soil concentrations for the Kosetice region, Czech Republic, from 1996 to 2005. They found decreasing concentrations for $\sum PAH_{16}$ as well as stronger declines for light PAH compared with heavy PAH.[9] The differing behaviour of light and heavy PAH in the Kosetice region resembles the observation made for Swiss sites, but declining trends of heavy PAH seem to be more pronounced for the Kosetice sites. The latter are located within the same region and thus represent a much smaller area than the Swiss monitoring sites. Possibly, in accordance with our site 33 (see above), the differences regarding trends of heavy PAH may be considered as regional phenomenon, although other reasons are possible as well, *e.g.* an even more pronounced decrease in emission of (heavy) PAH in the Czech Republic compared with Switzerland, soils and/or climatic conditions favouring degradation and volatilisation.

As stated above, we consider atmospheric deposition as main source of PAH found in Swiss background soils. The sediment profiles of Lake Thun[49] indicate slightly decreasing input fluxes over the last 30 years in the proximity of an urban area and stable input fluxes elsewhere for both heavy and light PAH. Hence, their results are in line with the evolutions found by the present study for heavy PAH, whereas the stable fluxes found for light PAH are contrasting with the decreasing concentrations observed in soils. Assuming that deposition rates are roughly proportional to the amount released into the atmosphere, emission inventories are a further database to assess the temporal evolution of PAH deposition. Inventory data for Switzerland indicate decreasing emissions for heavy PAH since the 1980s: total emissions of BaP, BbF, BkF, and IPY accounted for 21 t in 1980, reached a maximum of about 27 t in 1989 and thereafter steadily decreased to 6 t in 2012 (no data available for light PAH).[42] The decline is mainly attributed to the shutdown of primary aluminium production (2006), improved flue gas cleaning for waste incineration plants, and decreasing amounts of wood combusted in small scale firing places. Besides, foreign sources are relevant as well; for instance, estimates by the European Monitoring and Evaluation Programme (EMEP)[50] suggested that 50% of BaP depositions to Switzerland in 2013 were imported. However, imports are expected to decrease even faster than national emissions.[51] The temporal evolutions of PAH soil concentrations did not confirm the decreases in emissions suggested by inventory data. This might be either due to uncertainties of such inventories, or due to soil concentrations of heavy PAH reacting slowly to changing emissions.

3.5. Trends of molecular marker concentrations

The temporal evolutions of the marker substances (Fig. S8†) are of interest because they might provide evidence for the presence of specific PAH sources, although previous works showed the limitations of this approach.[18] As stated above, PER concentrations were decreasing, whereas cPHE, cPYR, COR, and RET generally showed constant concentrations. PER originates either from natural processes, particularly from the decay of plant material, or from combustion processes.[52] Due to the similarities with the evolutions of light PAH, it is assumed that the observed temporal evolutions of PER were caused by changing emissions from combustion processes. Different sources were suggested for the remaining markers: RET was attributed to the burning of conifer wood,[53,54] traffic emissions,[38] the decomposition of plant residues, and diagenetic processes.[55,56] COR was suggested as marker for traffic emissions, but comparable emissions were reported for biomass combustion.[57] And finally, cPHE and cPYR might originate from biomass burning as well as from traffic emissions.[38,54,58] However, due to strong correlations with heavy PAH, the found temporal evolutions do not allow for insights into the respective sources, except that non-anthropogenic sources seem improbable.

4 Conclusions and perspectives

The temporal evolutions of PAH in the top 20 cm of soils over 25 years indicate remarkably constant concentrations for heavy PAH. These findings disagree with inventory data suggesting declines in emissions of heavy PAH since the 1980s, but are in line with PAH input fluxes estimated for lake sediments. Regarding the persistence of medium to heavy PAH and the significant immissions prior to the studied period, it seems plausible that the PAH pools found by the present study are predominantly historic. In contrast, the contents of most light PAH declined – presumably as a result of decreasing PAH emissions in combination with loss processes, namely degradation, transport by water-flows and soil biota, and volatilisation. However, it remains unclear whether emissions decreased in general or for light PAH only. The combustion of wood produces relatively high portions of light PAH;[18] therefore, diminished amounts of wood burnt in small scale firings (as suggested by Primas *et al.*[59]) might explain the latter scenario. However, based on current knowledge, it seems more probable that the deviating trends for light and heavy PAH are attributable to their differing physico-chemical properties rather than to different groups of PAH emission sources showing divergent temporal trends (although a combination of both factors is possible). Light PAH react faster than their heavy analogues to changes in emissions due to their lower half-lifes in soils. In addition, their physico-chemical properties also induce rather diffuse (spatial) contamination, whereas those of heavy PAH favour more local contamination patterns. As a consequence, temporal trends within larger geographic regions are expected to be more uniform for light PAH compared with heavy PAH. Hence, NABO monitoring sites are expected to reflect more directly trends for light than for heavy PAH. Equally, the spatially differing evolutions observed for NAP and PHE might be explained by their physico-chemical properties. PAH inputs by other pathways than atmospheric deposition, in particular inputs *via* recycling fertilisers, seemed of minor relevance for the studied sites.

Future investigations may assess the following gaps in knowledge: (i) the bioavailability of PAH in soils,[60,61] (ii) the mobility and translocation of PAH in soils, *e.g.* by simultaneously analysing the evolutions in topsoil and subsoil, and (iii) the environmental behaviour of PAH in general, *e.g.* by using the presented data in modelling approaches.[9] In addition, comparable studies for further geographical locations and environmental conditions are highly desirable. Finally, we suggest revisiting the temporal evolutions at the sites assessed by the present study in the coming decades as, on the one hand, PAH emissions are expected to further decline over the next decade, but on the other hand, inputs *via* recycling fertilisers might increase as new products may enter the market and agricultural practice change.

Acknowledgements

The NABO is co-financed by the Federal Office for the Environment (FOEN) and Federal Office for Agriculture (FOAG). For the present study, we particularly acknowledge the hardware support by FOEN. Further, the authors thank Isabel Hilber (Agroscope) and Peter Schwab (NABO) for statistical and pedological discussions, Christian Bogdal (Agroscope & ETH Zurich) for helpful comments, and Sarah Grimm, Matteo Tanadini, and Werner Stahel (Seminar for Statistics, ETH Zurich) for statistical support. Finally, our thanks go to all past and present NABO collaborators for their contributions in soil sampling, preparation, and analyses.

References

1 WHO, *Health Risks of Persistent Organic Pollutants from Long-range Transboundary Air Pollution*, Copenhagen, 2003, p. 252.
2 K.-H. Kim, S. A. Jahan, E. Kabir and R. J. C. Brown, *Environ. Int.*, 2013, **60**, 71–80.
3 W. Wilcke, *Geoderma*, 2007, **141**, 157–166.
4 Y. Zhang and S. Tao, *Atmos. Environ.*, 2009, **43**, 812–819.
5 H. Shen, Y. Huang, R. Wang, D. Zhu, W. Li, G. Shen, B. Wang, Y. Zhang, Y. Chen, Y. Lu, H. Chen, T. Li, K. Sun, B. Li, W. Liu, J. Liu and S. Tao, *Environ. Sci. Technol.*, 2013, **47**, 6415–6424.
6 R. C. Brändli, T. D. Bucheli, T. Kupper, R. Furrer, W. A. Stahel, F. X. Stadelmann and J. Tarradellas, *J. Environ. Monit.*, 2007, **9**, 456–464.
7 T. Gocht, O. Klemm and P. Grathwohl, *Atmos. Environ.*, 2007, **41**, 1315–1327.
8 I. J. Keyte, R. M. Harrison and G. Lammel, *Chem. Soc. Rev.*, 2013, **42**, 9333–9391.
9 J. Komprda, K. Kubosova, A. Dvorska, M. Scheringer, J. Klanova and I. Holoubek, *J. Environ. Monit.*, 2009, **11**, 269–276.
10 I. Holoubek, L. Dusek, M. Sanka, J. Hofman, P. Cupr, J. Jarkovsky, J. Zbiral and J. Klanova, *Environ. Pollut.*, 2009, **157**, 3207–3217.
11 M. Trapido, *Environ. Pollut.*, 1999, **105**, 67–74.
12 E. J. Villanneau, N. P. A. Saby, T. G. Orton, C. C. Jolivet, L. Boulonne, G. Caria, E. Barriuso, A. Bispo, O. Briand and D. Arrouays, *Environ. Chem. Lett.*, 2013, **11**, 99–104.
13 D. J. Brus, F. P. J. Lame and R. H. Nieuwenhuis, *Environ. Pollut.*, 2009, **157**, 2043–2052.
14 J. J. Nam, G. O. Thomas, F. M. Jaward, E. Steinnes, O. Gustafsson and K. C. Jones, *Chemosphere*, 2008, **70**, 1596–1602.
15 B. Maliszewska-Kordybach, B. Smreczak, A. Klimkowicz-Pawlas and H. Terelak, *Chemosphere*, 2008, **73**, 1284–1291.
16 S. M. Rhind, C. E. Kyle, C. Kerr, M. Osprey, Z. L. Zhang, E. I. Duff, A. Lilly, A. Nolan, G. Hudson, W. Towers, J. Bell, M. Coull and C. McKenzie, *Environ. Pollut.*, 2013, **182**, 15–27.
17 A. Desaules, S. Ammann, F. Blum, R. C. Brändli, T. D. Bucheli and A. Keller, *J. Environ. Monit.*, 2008, **10**, 1265–1277.
18 R. C. Brändli, T. D. Bucheli, S. Ammann, A. Desaules, A. Keller, F. Blum and W. A. Stahel, *J. Environ. Monit.*, 2008, **10**, 1278–1286.
19 K. C. Jones, J. A. Stratford, P. Tidridge, K. S. Waterhouse and A. E. Johnston, *Environ. Pollut.*, 1989, **56**, 337–351.
20 K. C. Jones, J. A. Stratford, K. S. Waterhouse, E. T. Furlong, W. Giger, R. A. Hites, C. Schaffner and A. E. Johnston, *Environ. Sci. Technol.*, 1989, **23**, 95–101.
21 I. Holoubek, J. Klanova, J. Jarkovsky, V. Kubik and J. Helesic, *J. Environ. Monit.*, 2007, **9**, 564–571.
22 GEOSTAT Census 2013, Federal Statistical Office (FSO), Neuchatel, Switzerland, http://www.bfs.admin.ch/bfs/portal/de/index/news/04.html, accessed May 2015.
23 J. D. Berset, M. Ejem, R. Holzer and P. Lischer, *Anal. Chim. Acta*, 1999, **383**, 263–275.
24 T. D. Bucheli, F. Blum, A. Desaules and O. Gustafsson, *Chemosphere*, 2004, **56**, 1061–1076.
25 L. H. Keith, W. Crummett, J. Deegan, R. A. Libby, J. K. Taylor and G. Wentler, *Anal. Chem.*, 1983, **55**, 2210–2218.
26 W. Horwitz, *Anal. Chem.*, 1982, **54**, 67A–76A.
27 SETOC, http://www.wepal.nl/website/products/SETOC.htm, accessed June 2015.
28 D. Bates, M. Maechler, B. Bolker and S. Walker, *R Package lme4. Version 1.1–7*, 2014.
29 M. Hubert, P. J. Rousseeuw and K. Vanden Branden, *Technometrics*, 2005, **47**, 64–79.
30 V. Todorov and P. Filzmoser, *J. Stat. Software*, 2009, **32**, 1–47.
31 T. Hastie, R. Tibshirani and J. Friedman, *The Elements of Statistical Learning*, Springer, New York, 2nd edn, 2009.

32 R Development Core Team, *R: A Language and Environment for Statistical Computing, Version 3.1.2*, 2014.
33 D. Sarkar, *Lattice: Multivariate Data Visualization with R*, Springer, New York, 2008.
34 H. Wickham, *ggplot2*, Springer, New York, 2009.
35 B. H. Ellert and J. R. Bettany, *Can. J. Soil Sci.*, 1995, **75**, 529–538.
36 I. T. Cousins, H. Kreibich, L. E. Hudson, W. A. Lead and K. C. Jones, *Sci. Total Environ.*, 1997, **203**, 141–156.
37 I. T. Cousins, A. J. Beck and K. C. Jones, *Sci. Total Environ.*, 1999, **228**, 5–24.
38 T. Nielsen, H. E. Jorgensen, J. C. Larsen and M. Poulsen, *Sci. Total Environ.*, 1996, **189**, 41–49.
39 K. Kuoppamaki, H. Setala, A.-L. Rantalainen and D. J. Kotze, *Environ. Pollut.*, 2014, **195**, 56–63.
40 S. Y. N. Yang, D. W. Connell, D. W. Hawker and S. I. Kayal, *Sci. Total Environ.*, 1991, **102**, 229–240.
41 S.-D. Choi, C. Shunthirasingham, G. L. Daly, H. Xiao, Y. D. Lei and F. Wania, *Environ. Pollut.*, 2009, **157**, 3199–3206.
42 Federal Office for the Environment (FOEN), *Switzerland's Informative Inventory Report 2014*, Bern, 2014.
43 X. Liu, G. Zhang, K. C. Jones, X. D. Li, X. Z. Peng and S. H. Qil, *Atmos. Environ.*, 2005, **39**, 5490–5499.
44 J. D. Berset and R. Holzer, *Int. J. Environ. Anal. Chem.*, 1995, **59**, 145–165.
45 J. Marti, R. Bertini and M. S. Günthardt-Goerg, *Schweizerische Zeitschrift für Forstwesen*, 2015, 166, pp. 32–39.
46 Canton of Glarus, *Kataster des Ausstosses von Luftschadstoffen, Stand 2013*, Glarus, Switzerland, 2014.
47 R. E. Hester and R. M. Harrison, *Waste Incineration and the Environment*, Royal Society of Chemistry, Cambridge, England, 1994, vol. 2.
48 J. D. Berset, P. Kuehne and W. Shotyk, *Sci. Total Environ.*, 2001, **267**, 67–85.
49 C. Bogdal, T. D. Bucheli, T. Agarwal, F. S. Anselmetti, F. Blum, K. Hungerbuehler, M. Kohler, P. Schmid, M. Scheringer and A. Sobek, *J. Environ. Monit.*, 2011, **13**, 1316–1326.
50 European Monitoring and Evaluation Programme (EMEP), Country-specific report for Switzerland, http://www.msceast.org/index.php/switzerland, accessed June 2015.
51 A. Gusev, O. Rozovskaya, V. Shatalov, W. Aas and P. Nizzetto, *Persistent Organic Pollutants in the Environment, EMEP Status Report 3/2014*, 2014, http://www.msceast.org/reports/3_2014.pdf.
52 M. I. Venkatesan, *Mar. Chem.*, 1988, **25**, 1–27.
53 T. Ramdahl, *Nature*, 1983, **306**, 580–583.
54 B. R. T. Simoneit, *Appl. Geochem.*, 2002, **17**, 129–162.
55 T. P. Bastow, R. Alexander, S. J. Fisher, R. K. Singh, B. G. K. van Aarssen and R. I. Kagi, *Org. Geochem.*, 2000, **31**, 523–534.
56 L. Marynowski, J. Smolarek, A. Bechtel, M. Philippe, S. Kurkiewicz and B. R. T. Simoneit, *Org. Geochem.*, 2013, **59**, 143–151.
57 G. Shen, Y. Chen, S. Wei, X. Fu, A. Ding, H. Wu and S. Tao, *Environ. Pollut.*, 2014, **184**, 650–653.
58 E. Hedberg, A. Kristensson, M. Ohlsson, C. Johansson, P. A. Johansson, E. Swietlicki, V. Vesely, U. Wideqvist and R. Westerholm, *Atmos. Environ.*, 2002, **36**, 4823–4837.
59 A. Primas, L. Cloos and F. M. Kessler, *Schweizerische Holzenergiestatistik*, Bern, 2013.
60 X. Cui, P. Mayer and J. Gan, *Environ. Pollut.*, 2013, **172**, 223–234.
61 A. Cachada, R. Pereira, E. F. da Silva and A. C. Duarte, *Sci. Total Environ.*, 2014, **472**, 463–480.